Beyond the Standard Model in the Higgs sector

Elizaveta Cherepanova, on behalf of the ATLAS Collaboration
Nikhef National Institute for Subatomic Physics and University of Amsterdam, Science Park 105, 1098 XG Amsterdam, the Netherlands

The discovery of the Higgs boson with the mass of about 125 GeV completed the particle content predicted by the Standard Model. Even though this model is well established and consistent with many measurements, it is not capable to solely explain some observations. Many extensions of the Standard Model addressing such shortcomings introduce additional Higgs bosons, beyond-the-Standard-Model couplings to the Higgs boson, or new particles decaying into Higgs bosons. In this talk, the latest searches in the Higgs sector by the ATLAS experiment are reported, with emphasis on the results obtained with the full LHC Run 2 dataset at 13 TeV.

ATL-PHYS-PROC-2025-004
11 January 2025

1 Introduction

The Standard Model (SM) of particle physics shows good agreement with experimental observations but it still has quite a few unresolved issues. It does not suggest solutions for the strong Charge-Parity (CP) problem, the baryon asymmetry in the universe, dark matter, or the $(g-2)\mu$ anomaly. Some of these problems can be addressed with an extended Higgs sector, such as the Two-Higgs-Doublet Model (2HDM) and its modifications, including the 2HDM with an additional scalar boson S (2HDM+S), the Next-to-2HDM (N2HDM), and the General 2HDM with dropped Z_2 symmetry (g2HDM). Another promising framework is the Next-to-Minimal Supersymmetric Model (NMSSM).

These proceedings present four ATLAS searches for low- and high-mass resonances that probe the models listed above. The results are obtained using the full Run-2 dataset recorded by the ATLAS detector [1] at the LHC, with proton-proton collisions at a centre-of-mass energy of $\sqrt{s}$ =13 TeV.

2 Search for low-mass $X \to \gamma\gamma$

This search targets spin-0 resonances in the 66 to 110 GeV mass range with two photons in the final state [2]. Benchmark models include 2HDM, N2HDM, and NMSSM and the search utilizes both model-independent and model-dependent approaches. Events are categorized according to whether each photon converts or not, where in the model-dependent approach further categorization is done with a Boosted Decision Tree. The signal $m_{\gamma\gamma}$ distribution is modeled with a double-sided Crystal Ball (DSCB) function. Continuum non-resonant backgrounds $(\gamma\gamma, \gamma j, jj)$ are estimated with a two-dimensional sideband method, and the resonant Drell-Yan background $(Z \to ee)$ is modeled with a DSCB function.

The final signal yield is extracted from a fit to the $m_{\gamma\gamma}$ spectra. No significant excess over the SM expectation is observed. Upper limits at the 95% confidence level (CL) are derived for the fiducial cross-section times the branching ratio (BR) for the model-independent approach and for the total cross-section times the BR for the model-dependent approach (Figure 1). The largest deviations observed are at a mass of 71.8 GeV (95.4 GeV), with a local significance of 2.2σ (1.7σ) in the model-independent (model-dependent) approach.

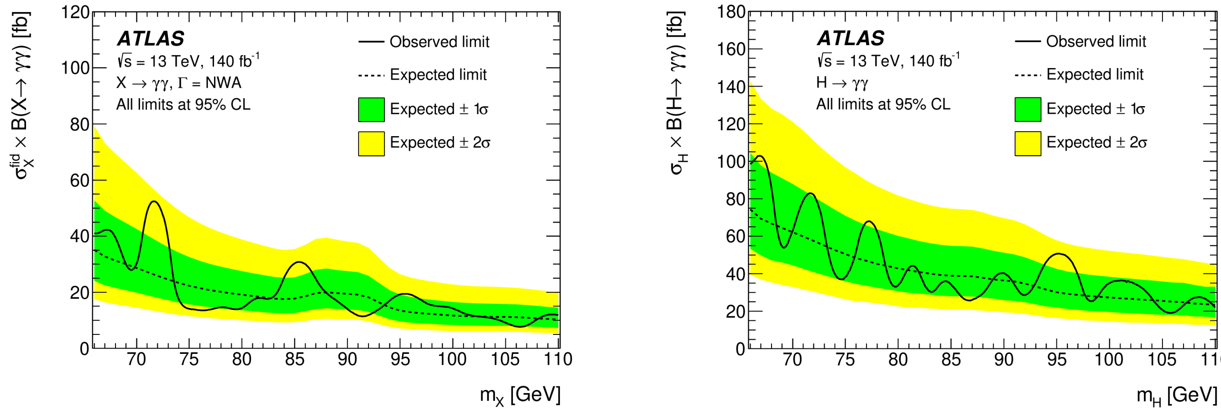

Figure 1 – Upper limits at 95% CL on the fiducial cross-section times BR $(X \to \gamma\gamma)$ as a function of the mass m_X assuming the narrow width approximation (left) and on the total cross-section times BR $(H \to \gamma\gamma)$ as a function of m_H (right). [2]

3 Search for $H \to aa \to 4\gamma$

This search targets the anomalous decay of a Higgs boson in the NMSSM model into two axion-like particles (ALPs) with four photons in the final state [3]. The mass m_a of the ALP is considered to be between 100 MeV and 60 GeV, and the ALP coupling to two photons $c_{a\gamma\gamma}$ between 10^{-5} TeV^{-1} and 1 TeV^{-1}. The search is divided into two categories: a search for long-lived particles (10^{-5} TeV^{-1} $< c_{a\gamma\gamma} <$ 0.1 TeV^{-1}), and a search for prompt decays (0.1 TeV^{-1} $< c_{a\gamma\gamma} <$ 1 TeV^{-1}). Main backgrounds ($h \to \gamma\gamma$ and multi-photon QCD) are estimated in sidebands of the mass distribution.

A simultaneous maximum-likelihood fit is performed on the mass distribution. No significant excess over the SM expectation is observed and upper limits are set on $B(H \to aa \to 4\gamma)$ at 95% CL (Figure 2). The largest deviation is observed in the range 10 GeV $< m_a <$ 25 GeV with a local significance of 1.2σ.

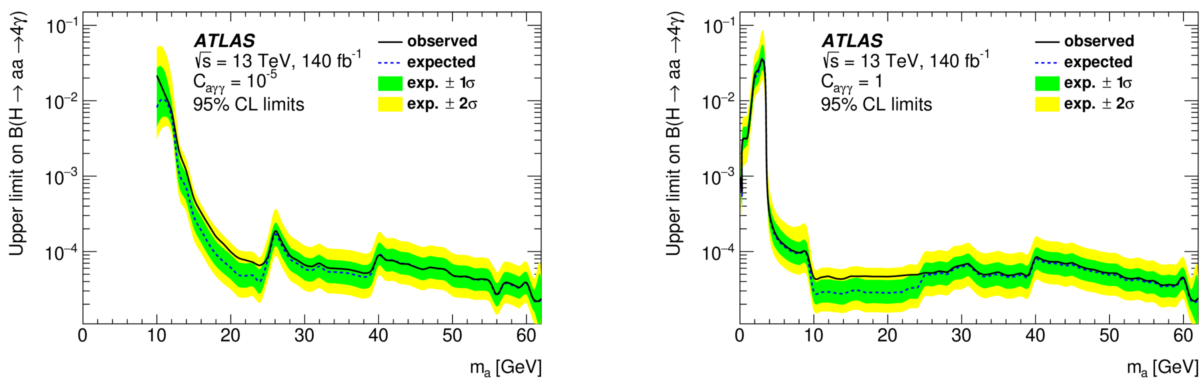

Figure 2 – Upper limits 95% CL on $B(H \to aa \to 4\gamma)$ as a function of m_a in a long-lived search (left) and in a prompt search (right). [3]

4 Search for heavy $H \to$ multi-l + b-jets

This search focuses on a heavy scalar that decays with same-sign top quarks in 2-, 3- and 4-top final states [4]. Leading-order Feynman diagrams for these processes are presented in Figure 3. Limits are set on two interpretation models, g2HDM and R-parity violating supersymmetry, but only the first one are covered in these proceedings.

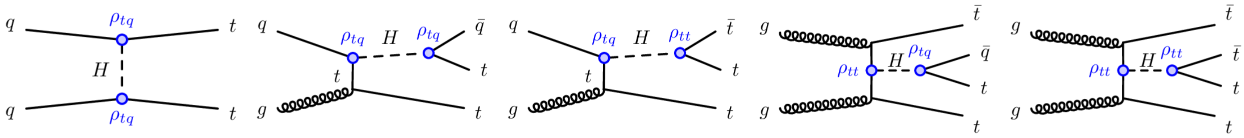

Figure 3 – Feynman diagrams for the dominant production and decay modes of the heavy scalar considered in the analysis. From left to right: same sign tt (sstt), ttq, ttt, tttq, tttt. [4]

Dedicated deep neural networks (DNN) classify events into five orthogonal decay regions and then split these according to their lepton multiplicity and total lepton charge. One classifier DNN^{cat} categorises events into different signal regions (SRs), another classifier DNN^{SB} separates signal-like and background-like events. Irreducible backgrounds ($t\bar{t}W$, VV, $t\bar{t}Z/\gamma^*$) are estimated using dedicated control regions. The reducible background from fake leptons is estimated via a template method, while the background from charge-flipped electrons is measured in the data using $Z \to ee$ decays.

A maximum-likelihood fit is performed on the DNN^{SB} score distribution in the SRs and on the number of b-jets, fake-lepton-candidate p_{T} and event yields in the control regions. No significant excess over the SM expectation is observed. Upper limits are set on the cross-section times BR at 95% CL for different coupling values. The upper limits for the scenario $\rho_{tt} = 0.4$, $\rho_{tc} = 0.2$, and $\rho_{tu} = 0.2$ are shown in Figure 4. This is the first limit on the g2HDM model from a collider experiment.

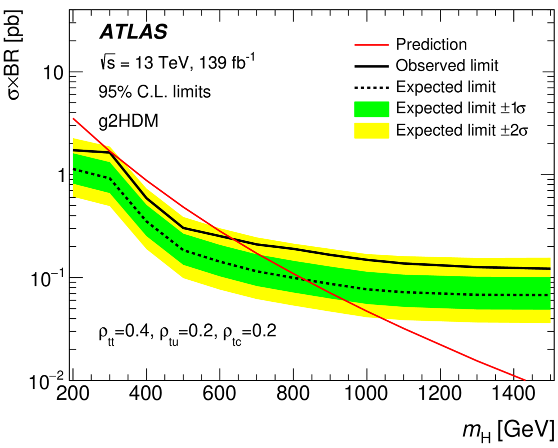

Figure 4 – Upper limit 95% CL on the heavy Higgs boson mass for g2HDM model and couplings $\rho_{tt} = 0.4$, $\rho_{tc} = 0.2$, and $\rho_{tu} = 0.2$. [4]

5 Search for $X \to 4l$ + MET/jets

This search targets heavy resonances with four leptons (e or μ) plus missing transverse momenta (E_{T}^{miss}) or jets in the final state, with interpretations in the 2HDM+S and 2HDM models [5]. Correspondingly, two different scenarios are studied. For the 2HDM+S interpretation, the scenario $R \to SH \to 4l + E_{\mathrm{T}}^{miss}$ is studied, where R and S are scalar bosons and S decays into dark matter particles, as shown in Figure 5 (left). For the 2HDM interpretation, the scenario $A \to ZH \to 4l+X$ is studied, where A is a CP-odd scalar with two possible decay combinations, as shown in Figure 5 (center and right). The masses of all bosons are considered within the following ranges: 390 GeV $< m_R <$ 1300 GeV, 320 GeV $< m_A <$ 1300 GeV, 220 GeV $< m_H <$ 1000 GeV, and $m_S = 160$ GeV. Linear interpolation is used to generate signal shapes between produced mass planes (m_R, m_H) and (m_A, m_H). The selection criteria for the signal regions is optimised based on the expected significance. Backgrounds ($q\bar{q} \to ZZ$, $gg \to ZZ$, VVV) are modelled using an empirical function.

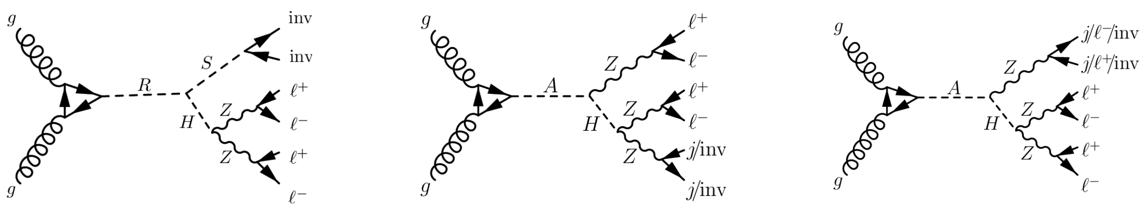

Figure 5 – Feynman diagrams representing the production of heavy bosons via gluon-fusion at leading order for the $R \to SH \to 4l{+}E_{\mathrm{T}}^{miss}$ (left), $A \to Z(\to 2l)H(\to 2l{+}jj/\text{invisible})$ (center), and $A \to Z(\to jj/l^+l^-/\text{invisible})H(\to 4l)$ (right) processes, where l represents an electron or a muon, j represents a jet and "inv" denotes an invisible particle. [5]

A binned maximum-likelihood fit is performed on the m_{ll} distrubution. No significant excess over the SM expectation is observed. Upper limits at 95% CL on the signal in the 2HDM+S and 2HDM models are set in the (m_R, m_H) and (m_A, m_H) mass planes, respectively, and are shown in Figure 6.

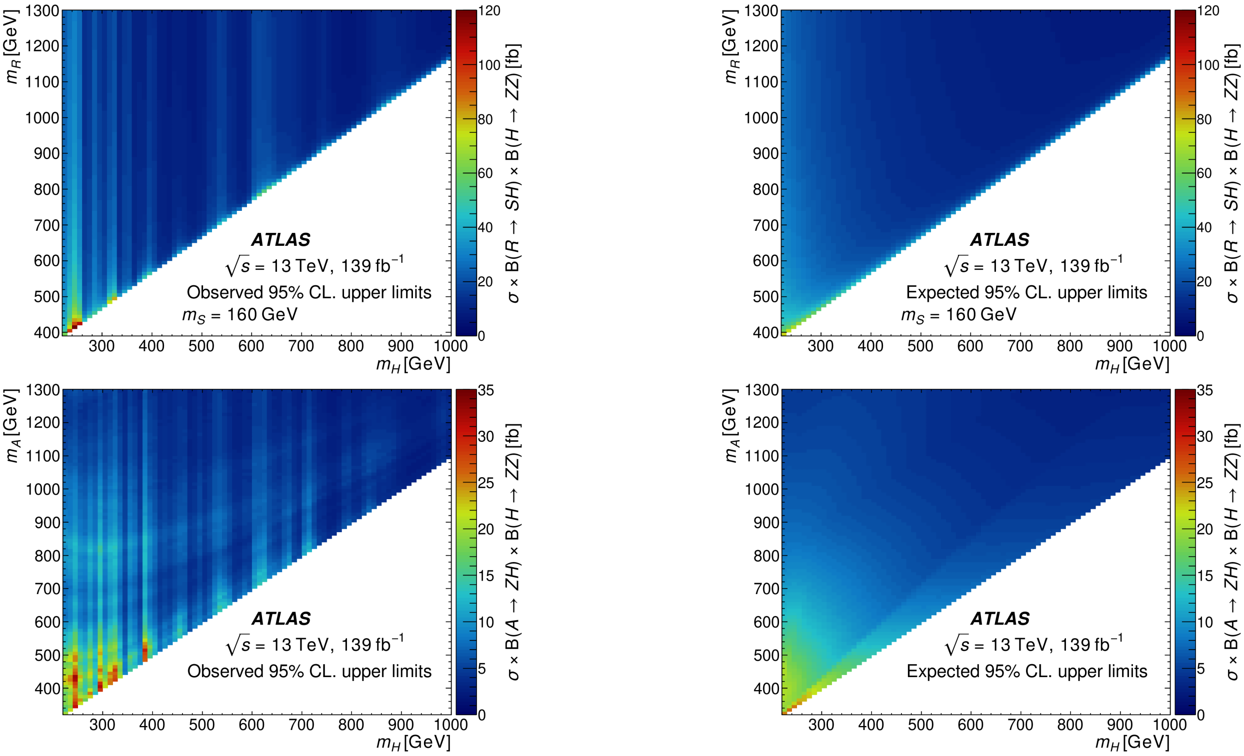

Figure 6 – The observed (left) and expected (right) upper limits at 95% CL on cross-section times BR across the (m_R, m_H) plane with $m_S = 160$ GeV for $R \to SH \to 4l + E_{\mathrm{T}}^{miss}$ search (top) and across the (m_A, m_H) plane for $A \to ZH \to 4l + X$ search (bottom). [5]

6 Summary and Outlook

These proceedings highlighted a selection of the latest results in the Higgs sector performed by the ATLAS Collaboration. While no significant deviations from the Standard Model have been observed to date, more searches are ongoing with Run-2 data. Data from the ongoing Run-3 of the LHC, as well as future data from the High Luminosity LHC will not only provide a significantly larger dataset but also allow for the exploration of additional production and decay channels.

References

1. ATLAS Collaboration. *The ATLAS experiment at the CERN Large Hadron Collider.* JINST **3**, S08003 (2008).
2. ATLAS Collaboration. *Search for diphoton resonances in the 66 to 110 GeV mass range using pp collisions at $\sqrt{s}$=13 TeV with the ATLAS detector.* Submitted to JHEP, arXiv:2407.07546
3. ATLAS Collaboration. *Search for short- and long-lived axion-like particles in $H \to aa \to 4\gamma$ decays with the ATLAS experiment at the LHC.* Eur. Phys. J. C **84**, 724 (2024).
4. ATLAS Collaboration. *Search for heavy Higgs bosons with flavour-violating couplings in multi-lepton plus b-jets final states in pp collisions at 13 TeV with the ATLAS detector.* JHEP **12**, 081 (2023).
5. ATLAS Collaboration. *Search for heavy resonances in final states with four leptons and missing transverse momentum or jets in pp collisions at $\sqrt{s}$=13 TeV with the ATLAS detector.* JHEP **10**, 130 (2024).